DERIVATION OF ELASTIC FRACTURE TOUGHNESS FOR DUCTILE METAL PIPES WITH CIRCUMFERENTIAL EXTERNAL CRACKS UNDER COMBINED TENSION AND BENDING

Chun-Qing Li[1,*], Guoyang Fu[1], Wei Yang[2] and Shangtong Yang[3]
[1]School of Engineering, RMIT University, Melbourne, Australia
[2]College of Engineering and Science, Victoria University, Melbourne, 8001, Australia
[3]Department of Civil & Environmental Engineering, University of Strathclyde, Glasgow, UK

ABSTRACT

Linear elastic fracture mechanics has been widely employed for fracture analysis of cracked pipes. For ductile metal pipes, the existence of plasticity eases the stress concentration at the crack front, which increases the fracture toughness of the pipe. Therefore, when using linear elastic fracture mechanics to predict the fracture failure of ductile pipes, the plastic portion of the fracture toughness should be excluded. This paper intends to derive an analytical model of elastic fracture toughness for ductile metal pipes with circumferential external surface cracks under combined axial tension and bending. The derived elastic fracture toughness is a function of crack geometry, material properties and loading conditions of the cracked pipe. The significance of the derived model is that the well established linear elastic fracture mechanics can be used for ductile materials in predicting the fracture failure. It is found in the paper that, the elastic fracture toughness increases with the increase of the internal pressure of the pipe and that an increase in fracture toughness and yield strength of the pipe materials will result in a more ductile and brittle pipe failure respectively. The derived analytical model enables more accurate prediction of fracture failure of ductile metal pipes with circumferential external cracks.

KEYWORDS

Fracture Toughness; Ductile material; Circumferential Crack; Plasticity; Stress Intensity Factor.

---

*Corresponding author: Professor Chun-Qing Li, Email: chunqing.li@rmit.edu.au

INTRODUCTION

Pipelines are essential infrastructure that play a pivotal role in a nation's economy, prosperity, health, environment, social well-being and quality of life. Various materials have been used to make pipes, a significant portion of which are ductile metals, e.g. steel. Due to their long term service and exposure to corrosive environment, aging and deterioration of metal pipes have resulted in failures well before the end of intended design life.

Through investigation, it has been found that most metal pipe failures are of fracture type, caused by the propagation of a surface crack or defect (Cabral and Kimber 1997; Rajeev et al. 2014). For cracked ductile metal pipes under applied loading, the crack front yields before the stress intensity factor reaches its critical value. This yielding eases the stress concentration at the crack front, and as a result, the fracture resistance, known as fracture toughness, increases. It follows that for ductile materials, fracture toughness of ductile materials should consist of elastic and plastic portions, with the latter contributed by the plasticity of the material. As is well known, most of fracture analysis is based on linear elastic fracture mechanics (LEFM), in which the materials do not reach the plastic stage. In order to make use of LEFM for ductile materials, the plastic portion of fracture toughness should be excluded from the overall or total fracture toughness. Otherwise the value of fracture toughness will be overestimated, resulting in an underestimated probability of pipe failure.

Extensive research has been conducted on calculating the stress intensity factors for surface cracks in pipes (e.g. Raju and Newman 1982; 1986; Mettu et al. 1992; Kou and Burdekin 2006; Li and Yang 2012). However, stress intensity factors thus obtained are only applicable to elastic materials and plastic materials under small scale yielding conditions (Anderson 1991). For ductile materials with large scale yielding, elastic-plastic parameters such as J integral (Rice 1968) and Crack Tip Opening Displacement (Burdekin and Stone 1966) have to be used. As such, non-linear finite element fracture analyses are often resorted to for investigating the behaviours of

cracked pipes made of ductile materials (e.g. Jayadevan 2004; Zhang et al. 2015), which requires more effort compared with elastic analyses. Further developments of the fracture mechanics based assessment led to the failure assessment diagrams, which are the most widely used methodology for elastic-plastic fracture analysis of structural components (Ainsworth 2003). Dowling and Townley (1975) identified two principal failure criteria, i.e., brittle fracture and plastic collapse, which is an essential step towards the development of failure assessment diagrams. These two criteria were then employed by Harrison et al. (1976) to define failure assessment diagram based on a modified strip yield model. Milne et al. (1988) presented detailed procedures for structural integrity assessment of ductile metal pipes with cracks, in which, failure assessment curves can be created based on the reference stress approach or elastic-plastic J integral analysis. Using their assessment method, the conditions of cracked pipes can be assessed by checking against the failure curves, with the consideration of both fracture and plasticity of pipe materials.

For fracture analysis of pipes made of ductile materials, if the portion of the fracture resistance within the elastic range can be determined, the widely available results based on linear elastic fracture mechanics can be readily applied. In this way, the simple criterion of stress intensity factor used in LEFM still applies. Literature review (see references) suggests that very little research has been carried out on distinguishing the elastic and plastic potions of fracture toughness for ductile materials. Yang et al. (2016) can be one of the first researchers that proposed an analytical model of elastic fracture toughness for steel pipes with internal cracks but that study is limited to internal longitudinal cracks under a single loading, i.e., internal pressure.

As is well known, the stress intensity factors are geometry and stress (loading) dependent. Although fracture toughness is a material property, it is also affected by geometry and loading once the material reaches plastic stage. Since pipes are frequently subjected to axial tension and bending in service, circumferential cracks often occur in pipes. As different cracks and loading

conditions may incur different failure modes, different analyses are required in deriving the elastic fracture toughness. This gives rise to the need for the present paper.

This paper aims to derive an analytical model of elastic fracture toughness for circumferentially cracked ductile pipes under combined axial tension and bending loads. The elastic fracture toughness in the derived model is a function of the geometry and material properties of the cracked pipe and applied loading. After verification of the derived model, parametric studies are conducted to investigate the effect of some key parameters on the elastic fracture toughness. The merit of the derived model is that it allows the use of extensive results based on linear elastic fracture toughness by engineers and asset managers for both design and assessment of ductile metal pipes, which can prevent future failures of pipes.

FORMULATION OF ELASTIC FAILURE TOUGHNESS

It is known that a cracked brittle pipe fails when the stress intensity factor K_I at the crack front exceeds the fracture toughness K_{IC}. For pipes made of ductile materials, plasticity develops at the crack front, which eases the stress concentration at the crack front. As a result, the fracture toughness increases. Consequently, the total fracture toughness should consist of two parts as follows

$$K_{Ic} = K_{IC}^{e} + K_{IC}^{p} \tag{1}$$

where K_{IC}^{e} is the elastic portion of the total fracture toughness K_{IC}, termed elastic fracture toughness, whereas K_{IC}^{p} is the plastic portion, referred to as plastic fracture toughness in this paper. To enable the use of LEFM for fracture analysis of ductile materials, K_{IC}^{e} can be extracted from the total fracture toughness and denoted as follows

$$K_{IC}^{e} = \alpha K_{Ic} \tag{2}$$

where α is defined as the ratio of the elastic fracture toughness to the total fracture toughness. By subtracting the elastic fracture toughness from Eq. (1), the plastic fracture toughness K_{IC}^{p} can be determined as follows

$$K_{IC}^{p} = (1-\alpha)K_{Ic} \tag{3}$$

With this separation, the following failure criteria in LEFM can still be used to assess the fracture conditions of ductile metal pipes

$$K_I \leq K_{IC}^{e} \tag{4}$$

Therefore, the key to the application of LEFM for ductile materials is to determine α.

For ductile metal pipes, failures often occur due to the interaction between two principal failure modes, i.e., brittle fracture and plastic collapse. Two parameters have been employed to quantify the two failure modes separately in the structural integrity assessment of cracked pipes as follows (Milne et al. 1988)

$$\begin{aligned} K_r &= K_I/K_{IC} \\ L_r &= P/P_L \end{aligned} \tag{5}$$

where P is the applied loading and P_L is the corresponding plastic load limit of the cracked pipes.

Based on experimental results, a relationship between K_r and L_r has been developed as follows (SINTAP 1999)

$$K_r = (1+0.5L_r^2)^{-0.5}[0.3+0.7\exp(-0.65L_r^6)] \tag{6}$$

where the maximum value of L_r is defined as $\overline{\sigma}/\sigma_y$, σ_y is the yield stress and $\overline{\sigma}$ is the uniaxial flow stress, calculated as the average of the yield and ultimate tensile strengths. Equation (6) has been widely used by researchers and practitioners as the failure assessment of cracked structures.

It needs to be noted that Equation (6) is the only relation between K_r and L_r as shown in literature (SINTAP 1999). Thus Equation (6) is employed as the basis for the derivation of the elastic fracture toughness for circumferentially cracked ductile metal pipes.

DERIVATION OF ELASTIC FRACTURE TOUGHNESS

Equation (6) establishes the relation among stress intensity factors K_I, fracture toughness K_{IC}, applied external loading P and plastic load limits P_L for cracked pipes. The Mode I fracture toughness of a certain metal K_{IC} can be determined using ASTM standard testing method (ASTM E1820-01). In this section, the formula for stress intensity factor K_I assuming linear elastic material are first derived by regression analyses based on finite element results. Then the analytical solution to plastic limit load P_L developed by Kim et al. (2003) is employed for circumferentially cracked pipes under combined axial tension and bending. Finally, the analytical model of elastic fracture toughness is developed with the consideration of different combinations of axial tension and bending.

Formula for Stress Intensity Factor (SIF). As it is known, the axial tension and bending forces only result in the opening mode (Mode I) fracture with a circumferential external surface crack in pipes (Figure 1). The Mode I SIFs for any point along the crack front can be expressed as follows (Raju and Newman 1982)

$$K_I = \sigma\sqrt{\pi\, a/Q}\, F_I(a/d\,, a/c\,, d/R_i\,, \varphi) \tag{7}$$

where σ is the applied stress, which can be σ_a induced by axial tension N or σ_b induced by bending M, a is the crack depth, Q is the shape factor for an ellipse, c is half crack length, d and R_i are the thickness and internal radius of the pipe respectively, φ is used to define the position along the semi-elliptical crack and F_I is the influence coefficient for Mode I fracture, as a function of the above parameters.

In order to obtain a general formula for pipes with circumferential surface cracks, three-dimensional finite element analyses are performed using ABAQUS (2011) to obtain SIFs for a wide range of crack and pipe geometries. The energy based *J*-integral method, which is path-independent and can produce accurate results with relatively coarse meshes, is employed. In addition, the meshing technique with mixed quadratic hexahedron and tetrahedron elements in Li et al. (2016) is adopted. Due to the free surface effect (Pook 1993), stress intensity factors at the surface points are estimated by extrapolation from the results close to the surface. As the critical values of SIFs occur either at the surface or deepest point along the crack front, only the results from these two locations are studied. Based on the finite element results, formulae of the influence coefficients of SIFs for circumferential cracks in pipes under axial tension and bending respectively are obtained by performing non-linear regression (MathWorks 2013) as follows

$$F_I(\cdot) = \{h_1 + h_2(a/c) + [h_3 + h_4(a/c) + h_5(a/c)^2](a/d)^2 + [h_6 + h_7(a/c) + h_8(a/c)^2]$$

$$(a/d)^4\}\exp(h_9(d/R_i)) \tag{8}$$

where the values of coefficient h_i ($i = 1, 2, \cdots, 9$) are listed in Table 1 for different loadings and geometries (a/c ranges from 0.4-1.5, a/d ranges from 0.2-0.8, and d/R_i ranges from 0.1-1). Equation (8) is within $\mp 6\%$ of the finite element results, which is sufficiently accurate for deriving K_{IC}^e.

For pipes under a combination of axial tension and bending, the SIFs can be calculated based on the principle of superposition (Anderson 1991)

$$K_I = \sqrt{\pi\, a/Q}\,[\sigma_a F_I(N) + \sigma_b F_I(M)] \tag{9}$$

where $F_I(N)$ and $F_I(M)$ are the influence coefficients for pipes under tension and bending respectively.

For pipes with a circumferential crack under axial tension N and bending M, the uniform axial stress σ_a and maximum bending stress σ_b can be represented as follows

$$\begin{aligned}\sigma_a &= \frac{N}{\pi\left(R_o^2 - R_i^2\right)} \\ \sigma_b &= \frac{4MR_o}{\pi\left(R_o^4 - R_i^4\right)}\end{aligned} \tag{10}$$

Substituting Equation (10) into Equation (9) yields the following

$$K_I = \sqrt{\pi\, a/Q}\left[\frac{N}{\pi\left(R_o^2 - R_i^2\right)} F_I(N) + \frac{4MR_o}{\pi\left(R_o^4 - R_i^4\right)} F_I(M)\right] \tag{11}$$

Plastic Limit Load. The majority of existing plastic load limits for pipes have been proposed either empirically based on piping testing data or analytically based on a simple yield criterion. These solutions tend to underestimate the actual limit load with unknown conservatism (Kim et al. 2002). For engineering assessment of cracked pipes, it is important to accurately determine the plastic limit loads. In this study, the analytical solution to the plastic load limit for pipe under combined axial tension and bending is employed. The solution was derived by Kim et al. (2003) based on stress fields equilibrium and improved by finite element limit analyses as follows

$$\frac{N}{2\pi\sigma_y R_m d}\frac{N_L'}{N_L} = 1 - \frac{a}{d}\frac{\theta}{4} - \frac{2\sin^{-1}\left(\frac{M}{4\sigma_y R_m^2 d}\frac{M_L'}{M_L} + \frac{af(\theta)}{d\ 2\theta}\right)}{\pi} \tag{12}$$

where $$N_L' = 2\pi\sigma_y R_m d\left[1 - \frac{a}{d}\frac{\theta}{4} - \frac{2\sin^{-1}\left(\frac{af(\theta)}{d\ 2\theta}\right)}{\pi}\right]$$

$$M_L' = 4\sigma_y R_m^2 d\left[\cos\left(\frac{\pi}{8}\frac{a}{d}\theta\right) - \frac{a}{d}\frac{f(\theta)}{2\theta}\right]$$

$$f(\theta) = 0.7854\theta^2 - 0.0982\theta^4 + 0.0041\theta^6 - 0.000085\theta^8$$

$$\theta = \frac{c}{R_m}$$

N_L is the plastic limit load for axial tension and given by

$$N_L = 2\pi\sigma_y R_i d\left[1 + A_1\left(\frac{a}{d}\right) + A_2\left(\frac{a}{d}\right)^2\right] \tag{13}$$

where $$A_1 = 0.066 - 0.038\left(\frac{\theta}{\pi}\right) - 0.960\left(\frac{\theta}{\pi}\right)^2$$

$$A_2 = -0.060 - 1.525\left(\frac{\theta}{\pi}\right) + 1.427\left(\frac{\theta}{\pi}\right)^2$$

M_L is the plastic limit load for bending and given by

$$M_L = 4\sigma_y R_i^2 d\left[1 + B_1\left(\frac{a}{d}\right) + B_2\left(\frac{a}{d}\right)^2\right] \tag{14}$$

where $$B_1 = 0.074 - 0.169\left(\frac{\theta}{\pi}\right)$$

$$B_2 = -0.086 - 1.013\left(\frac{\theta}{\pi}\right)$$

When the axial tension is constant, the plastic limit bending moment can be expressed as follows

$$M_L^N = 4\sigma_y R_m^2 d\frac{M_L}{M_L'}\left\{\sin\left[\frac{\pi}{2}\left(1 - \frac{a}{d}\frac{\theta}{4} - \frac{N}{2\pi\sigma_y R_m d}\frac{N_L'}{N_L}\right)\right] - \frac{a}{d}\frac{f(\theta)}{2\theta}\right\} \tag{15}$$

When the axial tension increases linearly with the bending moment, let the ratio of axial tension to bending moment be defined as follows

$$\xi = \frac{\sigma_a}{\sigma_b} = \frac{N\left(R_o^2 + R_i^2\right)}{4MR_o} \tag{16}$$

Substituting Equation (16) into Equation (12), the plastic limit bending moment can be obtained as follows

$$M_L^N(\xi) = 4\sigma_y R_m^2 d\frac{M_L}{M_L'}\left\{\sin\left[\frac{\pi}{2}\left(1 - \frac{a}{d}\frac{\theta}{4} - \frac{4M_L^N R_o\xi}{2\pi\sigma_y R_m d\left(R_o^2 + R_i^2\right)}\frac{N_L'}{N_L}\right)\right] - \frac{a}{d}\frac{f(\theta)}{2\theta}\right\} \tag{17}$$

whereas the corresponding plastic limit tension is as follows

$$N_L^M(\xi) = \frac{4M_L^N R_o \xi}{R_o^2 + R_i^2} \tag{18}$$

It should be noted that M_L^N in Equation (17) cannot be solved analytically and iterative methods such as Newton' method are needed.

Elastic Fracture Toughness for Circumferential External Cracks. For circumferentially cracked pipes under constant axial tension and varying bending moment, substitute Equations (11) and (15) into Equation (5) and it becomes

$$\begin{gathered} \frac{K_r K_{IC}\sqrt{\pi Q}\left(R_o^4 - R_i^4\right)}{\sqrt{a}} - N\left(R_o^2 + R_i^2\right)F_I(N) = 4MR_o F_I(M) \\ L_r = \frac{M}{M_L^N} = \frac{M}{4\sigma_y R_m^2 d\frac{M_L}{M_L'}\left\{\sin\left[\frac{\pi}{2}\left(1 - \frac{a\theta}{d4} - \frac{N}{2\pi\sigma_y R_m dN_L'}\right)\right] - \frac{af(\theta)}{d\ 2\theta}\right\}} \end{gathered} \tag{19}$$

In Equation (19), by dividing the first equation about K_r by the second equation about L_r, L_r can be expressed as follows

$$L_r = \frac{K_r K_{IC}\sqrt{\pi Q}\left(R_o^4 - R_i^4\right) - \sqrt{a}N\left(R_o^2 + R_i^2\right)F_I(N)}{4R_o\sqrt{a}F_I(M)\left\{4\sigma_y R_m^2 d\frac{M_L}{M_L'}\left\{\sin\left[\frac{\pi}{2}\left(1 - \frac{a\theta}{d4} - \frac{N}{2\pi\sigma_y R_m dN_L'}\right)\right] - \frac{af(\theta)}{d\ 2\theta}\right\}\right\}} \tag{20}$$

By solving Equations (6) and (20) simultaneously, the critical value of K_r at the fracture, denoted as K_{rc}, can be derived as follows

$$K_{rc} = \left(1 + 0.5\left(\frac{K_{rc} K_{IC}\sqrt{\pi Q}\left(R_o^4 - R_i^4\right) - \sqrt{a}N\left(R_o^2 + R_i^2\right)F_I(N)}{4R_o\sqrt{a}F_I(M)\left\{4\sigma_y R_m^2 d\frac{M_L}{M_L'}\left\{\sin\left[\frac{\pi}{2}\left(1 - \frac{a\theta}{d4} - \frac{N}{2\pi\sigma_y R_m dN_L'}\right)\right] - \frac{af(\theta)}{d\ 2\theta}\right\}\right\}}\right)^2\right)^{-0.5} \cdot$$

$$\left[0.3 + 0.7\exp\left(-0.65\left(\frac{K_{rc} K_{IC}\sqrt{\pi Q}\left(R_o^4 - R_i^4\right) - \sqrt{a}N\left(R_o^2 + R_i^2\right)F_I(N)}{4R_o\sqrt{a}F_I(M)\left\{4\sigma_y R_m^2 d\frac{M_L}{M_L'}\left\{\sin\left[\frac{\pi}{2}\left(1 - \frac{a\theta}{d4} - \frac{N}{2\pi\sigma_y R_m dN_L'}\right)\right] - \frac{af(\theta)}{d\ 2\theta}\right\}\right\}}\right)^6\right)\right] \tag{21}$$

Similarly, for circumferentially cracked pipes under combined axial tension and bending with a constant ratio, the relationship between K_r and L_r can be expressed as follows

$$L_r = \frac{\sqrt{\pi Q} K_r K_{IC}\left(R_o^4 - R_i^4\right)}{4\sqrt{a} R_o [\xi F_I(N) + F_I(M)] M_L^N(\xi)} \tag{22}$$

By solving Equations (6) and (22) simultaneously, the critical value K_{rc} of K_r for cracked pipes under bending at fracture can be derived as follows

$$K_{rc} = \left(1 + 0.5\left(\frac{\sqrt{\pi Q} K_r K_{IC}\left(R_o^4 - R_i^4\right)}{4\sqrt{a} R_o [\xi F_I(N) + F_I(M)] M_L^N(\xi)}\right)^2\right)^{-0.5} \cdot$$

$$\left[0.3 + 0.7 \exp\left(-0.65\left(\frac{\sqrt{\pi Q} K_r K_{IC}\left(R_o^4 - R_i^4\right)}{4\sqrt{a} R_o [\xi F_I(N) + F_I(M)] M_L^N(\xi)}\right)^6\right)\right] \tag{23}$$

where $\left\{\left(1 + 0.5\left(\frac{\overline{\sigma}}{\sigma_y}\right)^2\right)^{-0.5}\left[0.3 + 0.7 \exp\left(-0.65\left(\frac{\overline{\sigma}}{\sigma_y}\right)^6\right)\right]\right\} \leq K_{rc} \leq 1.$

When the critical state of pipe failure is reached, the stress intensity factor K_I for the brittle fracture will become the elastic critical limit, i.e., elastic fracture toughness K_{IC}^e, and K_{rc} becomes the ratio α defined in Equation (2). It follows that K_{IC}^e can be expressed as follows

$$K_{IC}^e = \alpha K_{IC} = K_{rc} K_{IC} \tag{24}$$

The plastic portion of the fracture toughness can be determined by subtracting the elastic portion in the total fracture toughness

$$K_{IC}^p = (1 - \alpha) K_{IC} = (1 - K_{rC}) K_{IC} \tag{25}$$

From Equations (21), (23) and (24), it can be seen that K_{IC}^e is a function of crack geometry, material properties and loading conditions of the cracked pipe. It should be noted that for engineering assessment elastic fracture toughness K_{IC}^e is the critical stress intensity factor

assuming the ductile metal pipe is brittle since the plastic behaviour of the metal pipes has been taken into account in deriving K_{IC}^{e}.

VERIFICATION AND DISCUSSIONS

To verify the derived elastic fracture toughness, ideally experimental results should be employed for comparison. However, a thorough literature review suggests that this is extremely difficult. Therefore, the derived model for elastic fracture toughness is verified indirectly by comparing K_r with data available in literature. Miller (1984) and Staat and Vu (2013) summarized the burst test results of pipes with circumferential cracks. A close inspection of the published data from literature reveals that very limited data can be used for verification purposes. Most cracks considered have very low aspect ratios, which are out of the applicable range of the stress intensity factor model, and for some tests, no specific material property data were documented. Schulze et al. (1980) carried out tests on steel pipes with both artificially and fatigue induced circumferential cracks of various lengths. The K_r value of the failed cracked pipes is calculated from the derived model, i.e., Equation (19), and the ASME boiler and Pressure code (1974), which was often used to interpret the experimental results of cracked pipes (e.g. Brown and Zybenko 1981). The results are shown in Table 2, from which it can be seen that satisfactory agreement has been achieved. The difference in the results might be caused by different finite element models employed and possible variation in determining and formulating the stress intensity factors K_I via non-linear regression respectively, as the same K_{IC} is used.

The results from Raju and Newman (1986) are also used for comparison of the stress intensity factors and good agreement has been achieved with a maximum difference of 5.8%. In addition, the plastic load limit has been verified by comparison with results from finite element fracture analyses (Kim et al. 2003) while Equation (6) has been derived as a lower bound of the failure assessment diagrams obtained based on the reference stress approach (SINTAP 1999), which will provide some safety margin for assessment.

Using the derived model, the structural failure of pipes with circumferential external surface cracks under combined tension and bending can be assessed by Equation (4), in which K_I and K_{IC}^e are calculated by Equations (11) and (24) respectively.

To demonstrate the application of the derived model for elastic fracture toughness, a pressurized pipe with closed ends under bending is taken as an example. In this case, the axial tension induced by internal pressure p is constant for given internal pressure. Consider a steel pipe with a circumferential external crack of $a/c = 0.4$, $a/d = 0.75$, $d/R_i = 0.1$ and $a = 3$. When the internal pressure p=10MPa, K_{rc} is 0.839 at the deepest point after solving Equation (21). From Equation (21), it can be seen that the constant axial tension affects the critical limit of K_r at fracture. Figure 2 shows the effect of the internal pressure induced tension force on the elastic fracture toughness. It can be seen that the elastic fracture toughness increases with the increase of the internal pressure of the pipe, which indicates that a higher internal pressure results in a smaller portion of fracture resistance offered by plastic deformation.

Equation (6) can be employed to plot the K_r-L_r curve for parametric study. For given cracked pipes under combined loading, K_r and L_r can be determined by Equations (20) or (22) for the deepest and surface points. In the following analyses, only the deepest points are considered. Similar analyses can be carried out for surface points, which are omitted here. From Equations (20) and (22), it can be seen that K_r and L_r exhibit a linear relationship for given combined loadings. For the case with constant aixal tension and varying bending , the amount of axial force controls the slope of the K_r-L_r line and the intersection point between the K_r-L_r line and the K_r axis. Take the internal pressure induced constant axial tension for example, as shown in Figure 3 a), increasing the internal pressure will decrease the slope of K_r-L_r line but will increase the K_r value at the intersection. When there is no internal pressure in the pipe, the K_r-L_r line starts from the origin. However, for the case with a constant ratio of axial tension and bending, the K_r-L_r line

is similar to the case under single loading, in which the line starting from origin as shown in Figure 3 b).

Figures 4 and 5 demonstrate the effect of material properties on failure mode at the deepest point for a given cracked pipe under bending and constant axial tension. The fracture toughness varies from 50 MPa$/\sqrt{\text{m}}$ to 110 MPa$/\sqrt{\text{m}}$ as shown in Figure 4 while the yield strength changes from 250MPa to 650 MPa as shown in Figure 5. It can be observed that for given pipe and crack geometry, the larger the fracture toughness of the pipe material is, the higher portion of plastic deformation the pipe will endure, which means the pipe will fail in a more plastic manner. This makes sense from both the theoretical analysis and practical observation. Similarly, the larger the yield strength of the pipe material is, the higher portion of the brittle fracture the pipe will offer, which indicates that the pipe will fail in a more brittle way. Again, this is consistent with practical experience.

Since the relative crack depth $a/d$is a critical factor that affects the pipe failure its effect on failure mode has also been investigated. As shown in Figure 6, when the relative depth increases from 0.2-0.8, the pipe material exhibits more brittleness. This can be explained by the amount of materials ahead of the crack front. Larger relative depth means less material to develop plastic deformation. Therefore, the pipe failure will tend to be at a lower level of plasticity.

CONCLUSIONS

An analytical model of elastic fracture toughness for ductile metal pipes with circumferential external surface cracks under combined axial tension and bending has been derived in this paper. The derived elastic fracture toughness is a function of crack geometry, material properties and loading conditions of the cracked pipe. One of the benefits for deriving elastic fracture toughness is that the well established linear elastic fracture mechanics can be used for ductile materials in predicting the fracture failure. It has been found in the paper that the elastic fracture toughness

306 increases with the increase of the internal pressure of the pipe, which indicates that a higher
307 internal pressure results in a smaller portion of fracture resistance offered by plastic deformation.
308 It has also been found that an increase in fracture toughness and yield strength of the pipe
309 materials will result in a more ductile and brittle pipe failure respectively and that an increase in
310 the relative crack depth will lead to less plastic deformation development in the pipe before
311 failure. It can be concluded that the derived analytical model enables more accurate prediction of
312 fracture failure of ductile metal pipes with circumferential external cracks.

313 **ACKNOWLEDGMENTS**

314 Financial support from Australian Research Council under DP140101547, LP150100413 and
315 DP170102211 is gratefully acknowledged.

NOMENCLATURE

a	depth of a semi-elliptical surface crack
A_1, A_2	coefficient functions for plastic limit load for axial tension
B_1, B_2	coefficient functions for plastic limit load for bending
c	half-length of surface semi-elliptical crack
d	wall thickness of a pipe
f	coefficient functions for plastic limit load
F_I	influence coefficient functions for Mode I
h_i	coefficients of influence coefficient functions
K_I	stress intensity factor for Mode I
K_{IC}	fracture toughness for Mode I
K_{IC}^e, K_{IC}^p	elastic and plastic fracture toughness for Mode I
K_r	ratio for measuring brittle fracture
K_{rc}	critical limit of K_r
L_r	ratio for measuring plastic collapse
M	bending moment
M_L, M_L'	plastic limit load for bending under Mises and Tresca conditions respectively
N	axial tension
N_L, N_L'	plastic limit load for axial tension under Mises and Tresca conditions respectively
p	internal pressure
P	applied external loading
P_L	plastic limit load of cracked pipes
Q	elliptical integral of the second kind
R_i, R_o, R_m	internal, external and mean radii of a pipe
α	ratio of the elastic fracture toughness to the total fracture toughness

341	θ	half of total crack angle for circumferential cracks, $\theta = c/R_m$
342	ξ	ratio of axial tension to bending moment
343	$\bar{\sigma}$	uniaxial flow stress
344	σ_a, σ_b	axial stresses induced by axial tension and bending respectively
345	σ_y	uniaxial lower yield stress
346	φ	position of a point along the semi-elliptical crack

347

REFERENCES

ABAQUS. (2011), Version 6.11 Documentation, Dassault Systèmes Simulia Corp., Providence, RI, USA.

Ainsworth, R.A., (2003), "7.03-Failure assessment diagram methods", Comprehensive Structural Integrity, 7, 89-132.

Anderson, T.L., (1991), "Fracture mechanics: fundamentals and applications", CRC Press, Boca Raton, Florida.

ASME Boiler and Pressure Vessel Code, (1974), "In service inspection of nuclear power plant components", section 11, Article A. 3000, p. 117.

ASTM E 1820-01, (2003), "Standard test method for measurement of fracture toughness", Pennsylvania, United States: ASTM International.

Brown, K.R. and Zybenko, B., (1981), "The fracture mechanics of aluminium alloy gas cylinders", Engineering Fracture Mechanics, 15, 1-20.

Burdekin, F.M. and Stone, D.E.W., (1966), "The Crack Opening Displacement Approach to Fracture Mechanics in Yielding Materials", Journal of Strain Analysis, 1, 145-153.

Cabral, M.A. and Kimber, M.J., (1997), "Pipeline fracture experiences in Australia and North America", APIA Symposium on Pipeline Fracture, Sydney, Australia, 10 August.

Dowling A.R. and Townley, C.H.A., (1975), "The effects of defects on structural failure: a two-criteria approach", International Journal of Pressure Vessels and Piping, 3, 77-107.

Harrison, R.P., Loosemore, K. and Milne, I., (1976), "Assessment of the Integrity of Structures Containing Defects," Central Electricity Generating Board report, R/H/R6, London.

Jayadevan, K.R., Østby. E., Thaulow. C., (2004), "Fracture response of pipelines subjected to large plastic deformation under tension", International Journal of Pressure Vessels and Piping. 81, 771-783.

Kim, Y.J., Shim, D.J., Huh, N.S. and Kim Y.J., (2002), "Plastic limit pressures for cracked pipes using finite element limit analyses", International Journal of Pressure Vessels and Piping, 79, 321-330.

Kim, Y.J., Shim, D.J., Huh, N.S. and Kim, Y.J., (2003), "Finite element based plastic limit loads for cylinders with part-through surface cracks under combined loading", International Journal of Pressure Vessels and Piping, 80, 527-540.

Kou, K. P. and Burdekin, F. M. (2006), "Stress intensity factors for a wide range of long-deep semi-elliptical surface cracks, partly through-wall cracks and fully through-wall cracks in tubular members", Engineering Fracture Mechanics, 73, 1693-1710.

Li, C.Q., Fu, G.Y. and Yang, W., (2016), "Stress intensity factors for inclined external surface cracks in pressurized pipes", Engineering Fracture Mechanics, 165:72-86.

Li, C.Q. and Yang, S.T. (2012), "Stress intensity factors for high aspect ratio semi-elliptical internal surface cracks in pipes", International Journal of Pressure Vessels and Piping, 96-97, 13-23.

MathWorks Inc. (2013), MATLAB R2013b. MathWorks, Inc., Natick, MA, USA.

Mettu, S. R., Raju, I. S. and Forman, R. G. (1992), "Stress intensity factors for part-through surface cracks in hollow cylinders", JSC Report 25685/LESC Report 30124, NASA Lyndon B. Johson Space Center/Lockheed Engineering and Sciences Co. Joint Publication.

Miller, A.G., (1984), "Review of test results for ductile failure pressure of cracked spherical and cylindrical pressure vessels", UK: CEGB.

Milne, I., Ainsworth, R.A., Dowling, A.R. and Stewart, A.T., (1988), "Background to and Validation of CEGB Report R/H/R6—Revision 3", International Journal of Presure Vessels and Piping, 32, 105-196.

Pook, L.P., (1995), "On fatigue crack paths", International Journal of Fatigue, 17(1), 5-13.

Raju, I.S. and Newman, J.C., (1982), "Stress-intensity factors for internal and external surface cracks in cylindrical vessels", Journal Of Pressure Vessel Technology-Transactions Of The ASME, 104(4), 293-298.

Raju, I.S. and Newman, J.C., (1986), "Stress intensity factors for circumferential surface cracks in pipes and rods", Fracture Mechanics: Seventeenth Volume, ASTM STP (Third Edn), 905, 789-805.

Rajeev, P., Kodikara, J., Robert, D., Zeman, P. and Rajani, B., (2014), "Factors contributing to large diameter water pipe failure", Water Asset Management International, 10(3), 9-14.

Rice, J.R., (1968), "A path independent integral and the approximate analysis of strain concentration by notches and cracks", Journal of Applied Mechanics, 35, 379-386.

Schulze, H.D., Togler, G. and Bodmann, E., (1980), "Fracture mechanics analysis on the initiation and propagation of circumferential and longitudinal cracks in straight pipes and pipe bends", Nuclear Engineering and Design, 58, 19-31.

Staat, M. and Vu, D.K., (2013), "Limit analysis of flaws in pressurized pipes and cylindrical vessels. Part II: Circumferential defects", Engineering Fracture Mechanics, 97, 314-333.

SINTAP, (1999), "Structural Integrity Assessment Procedures for European Industry—Final Procedure", European Union Project No.BE95-1426,

Yang, S.T., Li, C.Q. and Yang, W., (2016), Analytical model of elastic fracture toughness for steel pipes with internal cracks, Engineering Fracture Mechanics, 153, 50-60.

Zhang, Y.M., Yi, D.K., Xiao, Z.M., Huang, Z.H. and Kumar, S.B., (2013), "Elastic-plastic fracture analyses for pipeline girth welds with 3D semi-elliptical surface cracks subjected to large plastic bending", International Journal of Presure Vessels and Piping, 105-106, 90-102.

420 LIST OF TABLES

424

425

426

427 **Table 1** Values of coefficient h_i in Equation (8)

Coefficients	***Under tension***		***Under bending***	
	Deepest	*Surface*	*Deepest*	*Surface*
$\boldsymbol{h_1}$	1.086	0.550	0.999	0.566
$\boldsymbol{h_2}$	-0.052	0.568	-0.036	0.530
$\boldsymbol{h_3}$	2.168	-0.545	2.827	-0.038
$\boldsymbol{h_4}$	-3.898	2.518	-5.938	0.724
$\boldsymbol{h_5}$	1.680	-1.325	2.768	-0.290
$\boldsymbol{h_6}$	-1.778	0.942	-2.460	0.362
$\boldsymbol{h_7}$	3.667	-2.355	5.382	-0.600
$\boldsymbol{h_8}$	-1.708	1.183	-2.615	0.143
$\boldsymbol{h_9}$	0.046	0.021	0.109	0.059

428

429

430

431 **Table 2** Comparison of K_r for the deepest point between the derived model and those from the
432 ASME Boiler and Pressure code (1974)

R_i (mm)	a (mm)	$\frac{a}{c}$	$\frac{a}{d}$	K_{IC} (MPa/$\sqrt{\text{m}}$)	N (kN)	M (kNm)	K_r(ASME Boiler and Pressure code 1974)	K_r (Derived model)	Error (%)
33.5	3	0.25	0.75	98	0	9.1	0.84	0.80	5
33.5	3	0.25	0.75	98	35	8.2	0.85	0.78	8

433

434 LIST OF FIGURES

441

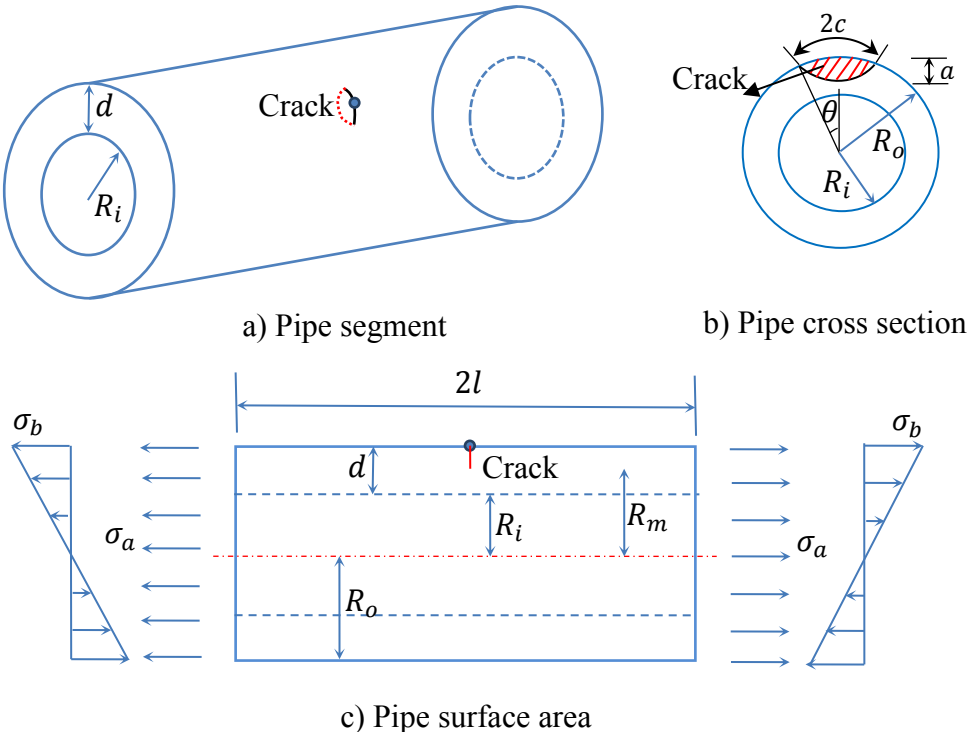

Figure 1 A pipe with a circumferential external surface crack subjected to axial tension and bending

448

449

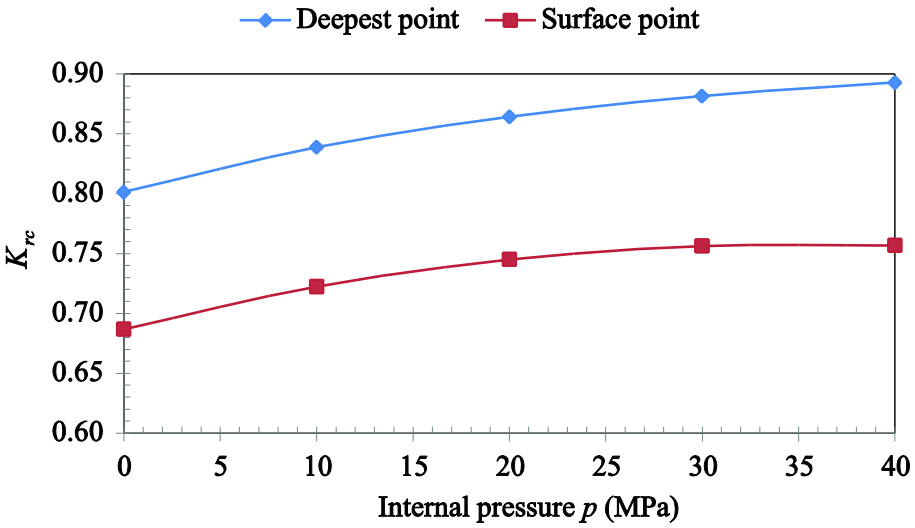

450

451 **Figure 2** Effect of internal pressure induced axial tension N on the K_{rc}

452

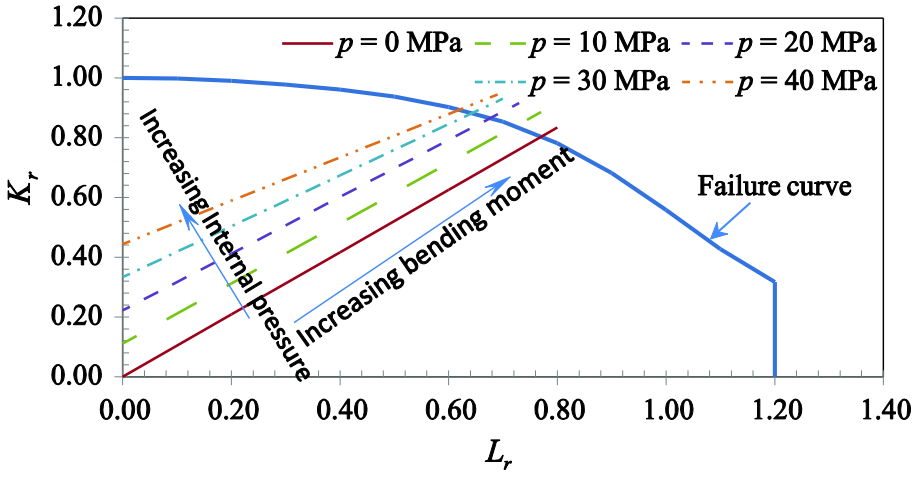

a) A pressurized pipe under bending

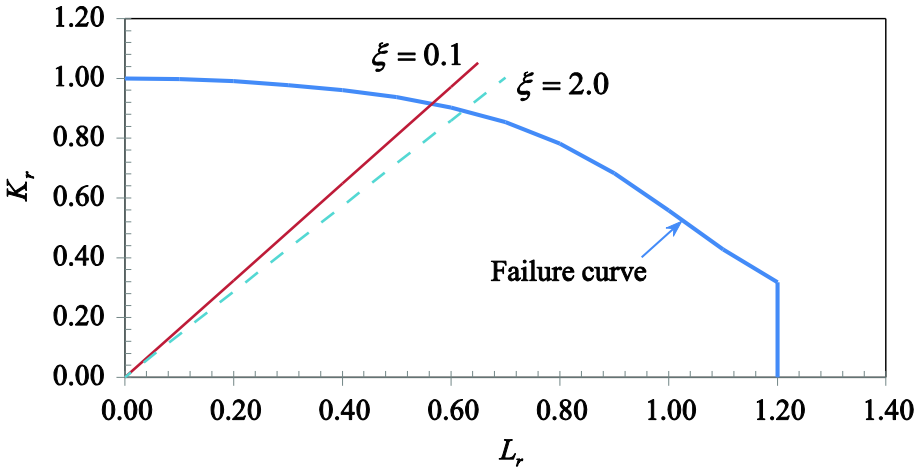

b) A pipe under combined axial tension and bending with a constant ratio

Figure 3 Failure assessment diagram for the deepest point

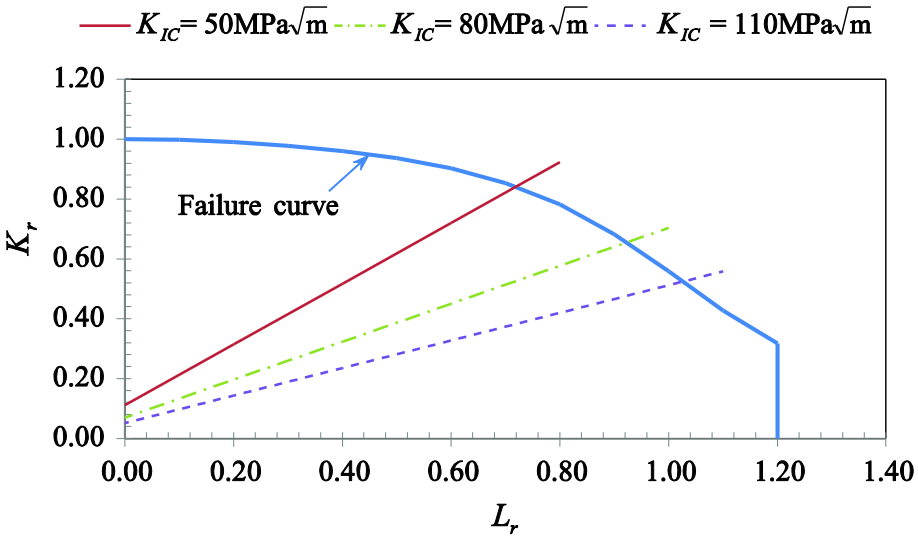

a) Case with constant axial tension and varying bending

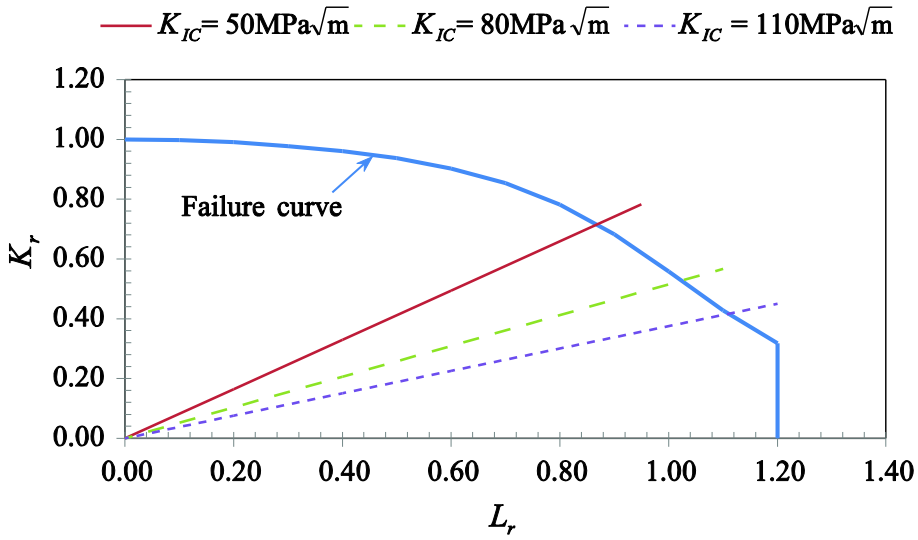

b) Case with a constant ratio of axial tension to bending

Figure 4 Effect of fracture toughness on pipe failure at the deepest point

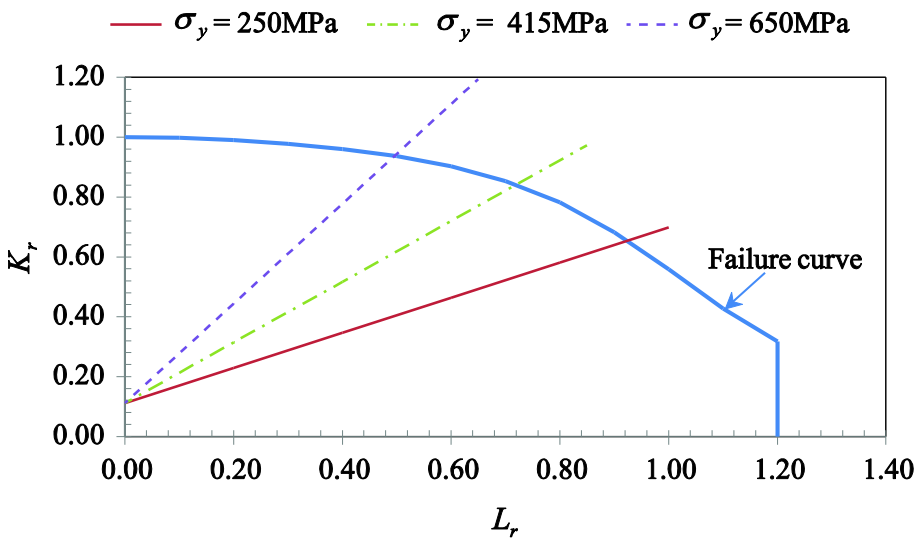

a) Case with constant axial tension and varying bending

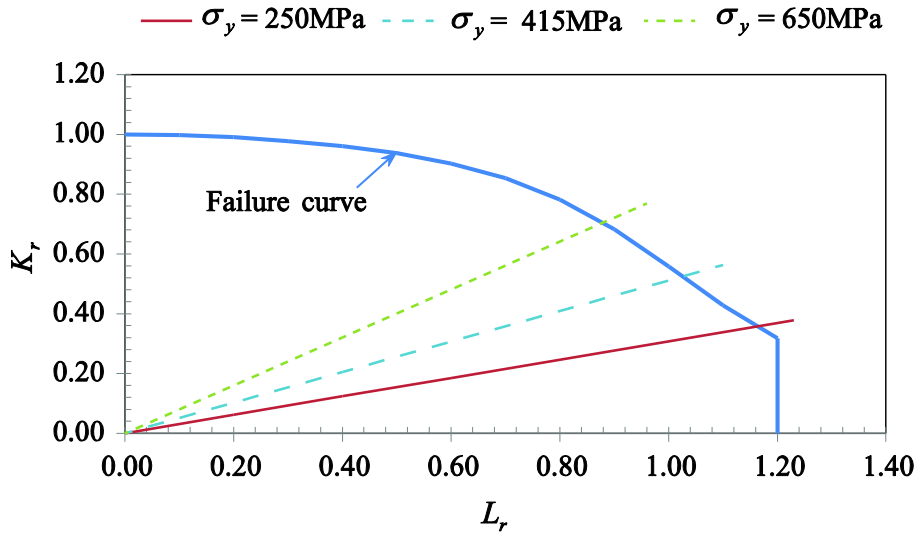

b) Case with a constant ratio of axial tension to bending

Figure 5 Effect of yield strength on pipe failure at the deepest point

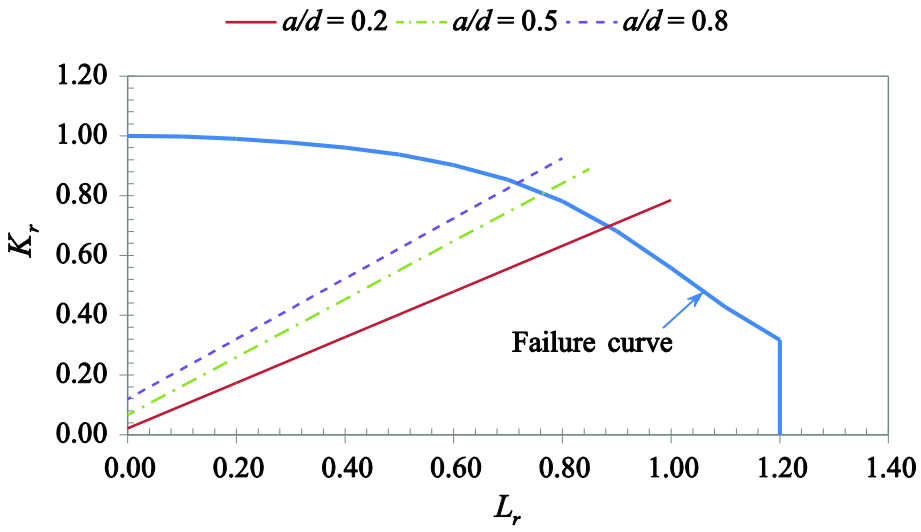

a) Case with constant axial tension and varying bending

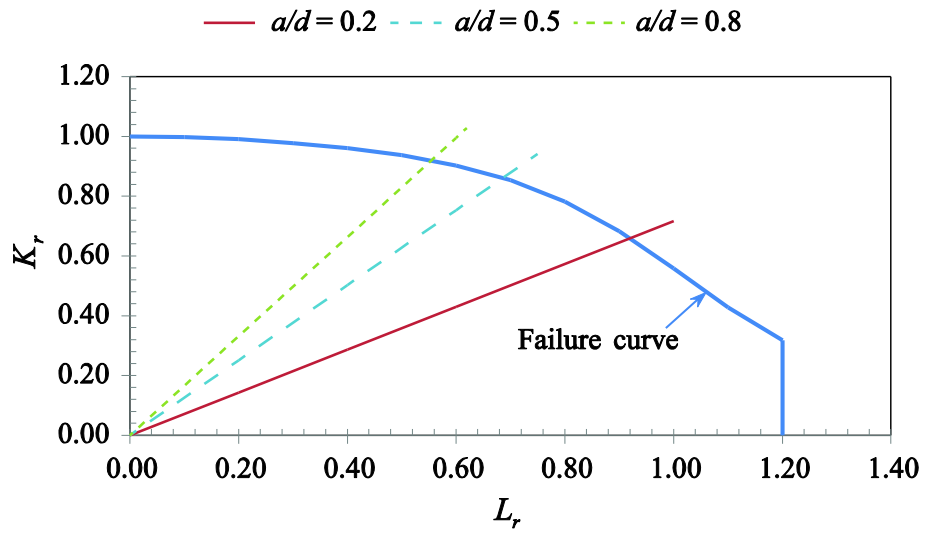

b) Case with a constant ratio of axial tension to bending

Figure 6 Effect of relative crack depth a/d on pipe failure at the deepest point

y